

Wakefield assisted bunch compression in storage rings

Sergey A. Antipov, Ilya Agapov, Igor Zagorodnov and François Lemery

Deutsches Elektronen-Synchrotron DESY, Notkestr. 85, 22607 Hamburg, Germany

E-mail: Sergey.Antipov@desy.de

ABSTRACT: Equilibrium bunch lengths typical to modern day light sources of tens of picoseconds limit the spectral reach of superradiant approaches for exploring materials and biological samples. In particular, generation of terahertz radiation seems appealing for pump-probe experiments. Taking advantage of self-wakes generated by carefully chosen structure one can control the bunch length and shape the bunch profile to increase significantly the high-frequency spectral components. Numerical analysis indicates the presence of self-consistent steady states that can be obtained with passive corrugated or dielectric structures. This approach has potential applications for generating superradiant terahertz radiation and pulse shaping in circular accelerators.

KEYWORDS: Beam dynamics, Accelerator applications

¹Corresponding author.

Contents

1	Introduction	1
2	Bunching for single-mode wakes	2
2.1	Stationary distribution for a single-mode wake	2
2.2	Stability limitations	3
3	Numerical simulation setup	4
4	Results and Discussion	5
4.1	Single-mode structure	5
4.2	Corrugated slab structure	5
4.3	KARA ring example	6
4.4	PETRA IV ring example	9
5	Radiation generation	10
6	Conclusion and Outlook	12

1 Introduction

Beyond the production of X-rays in storage rings, terahertz (THz) and mid-infrared (MIR) radiation generation has been widely explored, especially in the context of coherent synchrotron radiation. Early observations indicated that by driving a machine toward the microwave instability (MWI), large broadband and coherent bursting would occur under suitable conditions [1–3]. In parallel, the design of low-momentum-compaction (low- α) storage rings were developed to support bunch lengths comparable to the desired radiation wavelength produced in a bending magnet [4]. In addition a low-energy storage ring dedicated to THz generation was proposed [5]. Recently feedbacks were employed to maintain a microbunching structure on the beam, allowing the production of stable coherent radiation [6]. THz radiation generation at an energy recovery linac has also been investigated; the smaller achievable bunch lengths in such a platform are favorable to reach larger frequencies and enable the production of large average powers [7].

These techniques all rely on bending magnets e.g. synchrotron radiation to produce THz/MIR, and are generally broadband. Alternatively in the linear accelerator community, there has been tremendous interest in Cherenkov waveguides, e.g. dielectric-lined (DLW), corrugated, or bimetallic waveguides for beam manipulation diagnostics and radiation generation. Beam manipulation studies have especially shown and demonstrated techniques to microbunch beams or to more generally synthesize longitudinal phase spaces [8–12]. These effects can be used to enhance the bunch form factor to couple more strongly to similar waveguides which can in turn radiate more

energy. Large field gradients (GV/m) have been demonstrated in the superradiant regime where the form factor is approximately unity [13]. For a comprehensive discussion on superradiant radiation generation in Cherenkov structures, see ref. [14]. We note that a recent technique to characterize such waveguides has been developed [15].

In this paper we investigate the use of Cherenkov waveguides in storage rings. While it is well known that introducing impedances can modify the equilibrium bunch length [16–18], here we further study this feature to longitudinally squeeze the equilibrium bunch length by adiabatically increasing the wakefield amplitude in a corrugated planar structure. The scheme is investigated with analytical and numerical considerations and backed with particle tracking simulations. We demonstrate how the equilibrium bunch distribution can be modified in a controlled way by means of a compact Cherenkov waveguide structure and also discuss limitations of this approach with regards to beam stability. Finally, we also investigate using a secondary wakefield structure to produce radiation with the new equilibrium bunch length.

2 Bunching for single-mode wakes

2.1 Stationary distribution for a single-mode wake

Consider a relativistic electron bunch orbiting in a storage ring. Let the number of particles in a bunch be N_b , the revolution frequency f_0 , and γ the Lorentz factor. Let us further assume a quadratic rf potential well, in which the particles oscillate with an angular synchrotron frequency ω_s . Below the microwave instability threshold the normalized stationary longitudinal bunch distribution ρ in the presence of a wakefield W' is described by the Haissinski integral equation [16]:

$$\begin{aligned} \frac{\rho(\xi)}{\rho_0(\xi)} &\propto \exp \left[\kappa \int_0^\xi \int_{\xi''}^\infty \rho(\xi') w'(\xi'' - \xi') d\xi' d\xi'' \right], \\ \rho_0(\xi) &= \frac{1}{\sqrt{2\pi}} \exp \left[-\frac{\xi^2}{2} \right], \end{aligned} \quad (2.1)$$

where $\xi = z/\sigma_{z0}$ stands for the normalized coordinate, σ_{z0} is the zero intensity rms bunch length, and the normalization condition is $\int \rho(\xi) d\xi = 1$. The normalized wake force is $w'(\xi) = W'(\xi)/W_0$, $W_0 = W'(0)$. The coupling strength is $\kappa = W_0 \frac{\alpha f_0 c}{\gamma \omega_s^2} \frac{N_b r_0}{\sigma_{z0}}$; c is the speed of light and r_0 the classical electron.

Eq. (2.1) can be solved analytically for certain special wakes [17–20]. One can see that some wakes can create additional longitudinal focusing, reducing bunch length. Longitudinal focusing has been shown, for example, for a purely inductive wake [18], a purely capacitive wake [20–22], and for a wake of a ferrite-lined waveguide [23]. In this paper we consider short-range wakes that can be easily generated in the ring with the help of corrugated or dielectric waveguide structures. This approach seems promising as waveguide structures can be readily engineered to have the desired frequency content in their wakefield and are capable of generating relatively large wakefields over a short distance. As an example consider a Gaussian distribution $\rho(z)$ and a cosine wake $W'(z) = W_0 \cos(2\pi z/\lambda)$. Then for $\lambda \sim \sigma_z$ the convolution of the wake with the bunch density creates a longitudinal potential well with the dimensions comparable to σ_z (Fig. 1). The particles in the head lose energy, while the particles in the tail gain, and the total energy loss

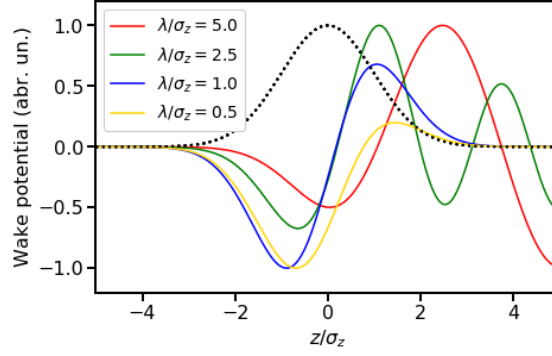


Figure 1. Normalized wake potential for different ratios of the structures frequency to the rms bunch length λ/σ_z for a Gaussian bunch profile (depicted by the dotted black line).

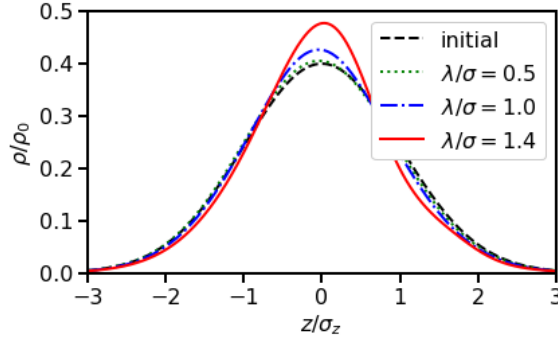


Figure 2. Normalized bunch distributions after compression with a cosine-like wake for different wake wavelengths, found as solutions of Eq. (2.1). Normalized wake potential $\kappa = 18$. The unperturbed distribution is shown in black.

by the bunch is minimal. For negligibly weak wakes the solution of Eq. (1) is simply a normal distribution: $\rho(\xi) = \rho_0(\xi) = \frac{1}{\sqrt{2\pi}} \exp\left[-\frac{\xi^2}{2}\right]$. As W' increases it produces an extra focusing that reduces the bunch length. In order to obtain the final stationary distribution one can start with a normal distribution and solve Eq. (1) iteratively. Figure 2 presents examples of resulting bunch shapes for different wake wavelengths.

2.2 Stability limitations

Eq. (1) only holds below the MWI threshold. Above the threshold both the bunch length and momentum spread increase thereby limiting the maximum bunch compression that can be achieved with a passive structure. For resonator-like wakes¹ the MWI threshold current for a Gaussian bunched beam can be found from [24]

$$I_{th} = F \times \frac{\alpha(E/e)\delta_{p,FWHM}^2}{|Z/n|}, \quad (2.2)$$

where E and e stand for the beam energy and electron charge respectively, F is a form factor, α is the momentum compaction factor, and $|Z/n|$ is the effective longitudinal impedance. The second part of

¹Note that Eq. (2.2) does not apply for some special cases, such as a purely capacitive or a purely resistive wake.

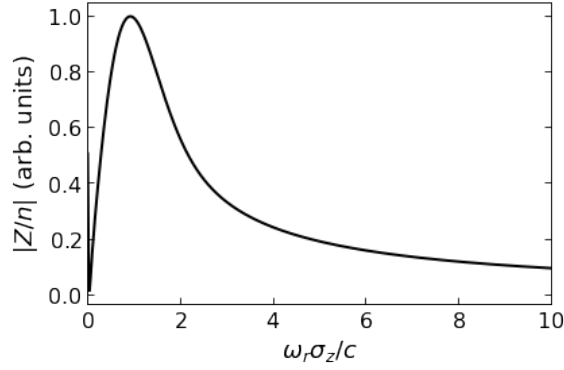


Figure 3. Effective impedance Z/n of a narrow-band resonator as a function of its normalized frequency.

the product represents the Keil-Schnell-Boussard stability criterion [25], which in case of bunched beams has to be computed with local densities of bunch current I and full-width-at-half-maximum relative energy spread $\delta_{p,FWHM}$. For wakes with $\lambda \sim \sigma_z$, $F \approx 1$.

The effective impedance is defined as

$$|Z/n| = \int_{-\infty}^{+\infty} Z(\omega) \frac{\omega_0}{\omega} h(\omega) d\omega, \quad (2.3)$$

where $h(\omega)$ is the normalized beam power spectrum, $\int_{-\infty}^{+\infty} h(\omega) d\omega = 1$ and $\omega_0 = 2\pi f_0$. For a Gaussian bunch spectrum $h(\omega) \propto \exp(-\omega^2 \sigma_z^2 / c^2)$ and an impedance peaked at an angular frequency ω_r , the $|Z/n|$ maximizes when $\omega_r \sigma_z / c = 1$ (Fig. 3). Thus, increasing the frequency of the impedance seems beneficial for mitigating the instability, potentially achieving larger bunch compression.

It shall be noted as well that in a real machine the instability can be mitigated with other measures, i.e. employing a longitudinal feedback or increasing the momentum spread with an undulator. Thus, Eq. (2.2) does not necessarily represent a strong limit on the practically achievable bunch compression.

3 Numerical simulation setup

In order to assess the effect numerically we performed particle tracking studies using a 1D macroparticle tracking code, where the relativistic electron beam is represented as an ensemble of $N = 10^5$ macroparticles. The code treats the ring as a transfer map with an rf and a wake kick. In order to compute the wake kick the beam is sliced into 100 longitudinal slices, a smooth current density function is computed from the discrete number of particles in each slice using a 2nd order Savitzky–Golay filter, and finally a convolution with the Green’s function of the wake is computed.

The initial distribution was assumed to be a 1D Gaussian. We neglected other effects that might also affect the longitudinal distribution in a real machine, like intra-beam scattering, synchrotron radiation damping, or coherent synchrotron radiation. The complete longitudinal wakefield was assumed to be created by the structure alone with no other sources of beam coupling impedance considered. This was done with the sole purpose of simplifying the model and assessing the limits of the proposed approach separately.

4 Results and Discussion

In practice there are several ways of generating the desired wake potential in the ring. Here we first consider a fixed aperture dielectric cylindrical waveguide (DLW) that can be treated as a single-mode structure. We also consider a variable gap corrugated structure.

4.1 Single-mode structure

To gain insights into the beam dynamics and stability of this configuration, we implemented a cylindrically-symmetric DLW with wake potential $W'(z) = W_0 \cos(2\pi z/\lambda)$. Here the transverse parameters, e.g. inner radius and dielectric thickness determine the spectral content of the waveguide while the structure length determines the strength of the produced wake [26, 27]. The wakefields were numerically implemented using publicly available PYTHON scripts [28].

Considering $\lambda/\sigma_z = 0.8$ and a moderately high normalized wake strength $\kappa = 36.12$ (Example parameters: radius of 5 mm, 7 μm coating with a dielectric permittivity of 10 for a 400 GHz structure) we observe a measurable bunching of the initial Gaussian distribution in our tracking (Fig. 4). The peak current density increases by $\sim 10\%$. This result is in excellent agreement with the prediction of Eq. (2.1) for the considered wake.

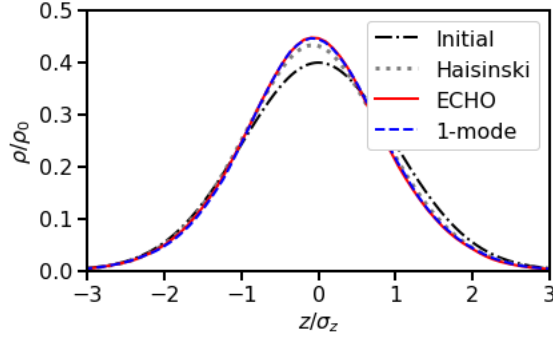


Figure 4. Below the microwave instability threshold the predictions of the Haisinski equation (blue dots) match well the tracking results for a single-mode dielectric structure (orange line) and a corrugated slab structure that creates generates the same wake potential (green line). Wavelength of the 1-mode structure $\lambda/\sigma_z = 0.8$, normalized wake strength $\kappa = 36.12$. The initial distribution is shown in black.

Larger peak currents can be achieved by increasing the wakefield strength until the MWI threshold. This limit was explored numerically, we first implemented an unperturbed Gaussian distribution and then adiabatically increased W_0 in small increments. The peak density increased quasi-linearly until $\kappa \sim 75$, where the bunch started exhibiting unstable behaviour and subsequently rapidly expanded and reduced its peak density; see Fig. 5. Larger λ helps bunching the beam more efficiently, requiring less wakefield strength, but limits the maximum achievable bunch compression to smaller values.

4.2 Corrugated slab structure

In practice it is convenient to generate the required wakefield with a variable-gap slab structure. In addition, slab-structures are advantageous, especially with flat-beams, to mitigate dipole mode

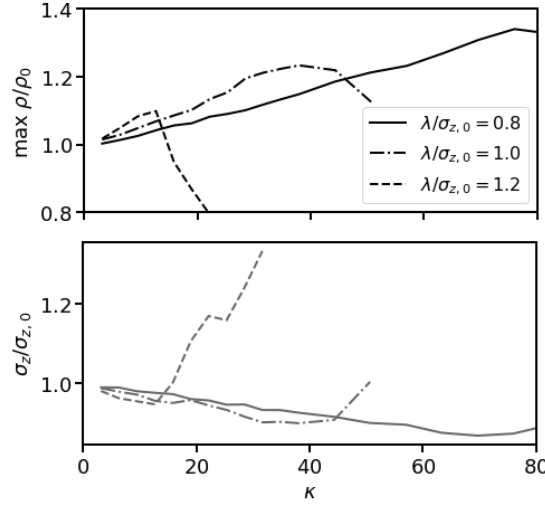


Figure 5. Normalized peak current (a) and bunch length (b) as a function of the normalized strength parameter κ for $\lambda / \sigma_{z,0} = 1.2$, $\lambda / \sigma_{z,0} = 1.0$, and $\lambda / \sigma_{z,0} = 0.8$. A shorter wavelength requires a larger wake to achieve the same level of bunch compression, but at the same time allows compressing the bunch further.

excitations which can destabilize the beam [29]. In such a structure the period and the depth of corrugations mainly govern the resonance frequency while the size of the aperture largely affects the wake strength. Figure 6a shows an example of such a structure, designed to have a resonance frequency f_r about 400 GHz. The corresponding longitudinal impedance, obtained from ECHO [30], is shown in Fig. 6b; at lower frequencies it can be well approximated with a single-mode broad-band resonator:

$$Z(f) = \frac{R_s}{1 + iQ(f/f_r - f_r/f)}, \quad (4.1)$$

where R_s stand for the resonator shunt impedance and Q for its quality factor. Performing the particle tracking for the same wake strength $\kappa = 36.12$ as in the single-mode case we obtain an identical final beam distribution (Fig. 4). Thus, for a realistic impedance under the MWI threshold the results agree with the theoretical predictions and the simplified single-mode-structure model.

4.3 KARA ring example

As a practical example, we have studied numerically the extent of achievable bunch shortening at a low- α KARA ring at KIT. The 110-m-long ring is capable of circulating electron bunches of 370 – 740 pC and rms bunch length of 2 – 10 ps (Table 1). It has a 40-cm-long straight section suitable for an installation of a passive dielectric or corrugated structure. The β -function in the straight section and orbit tolerances limit the aperture of the structure to 5 mm. We have considered two cases: a machine operating at $\alpha = 5 \times 10^{-4}$ with 3 ps rms bunches and a lattice with a larger momentum compaction of 8×10^{-3} with 10 ps rms bunches.

First, let us consider the later case of $\alpha = 8 \times 10^{-3}$, $\sigma_{z,0}/c = 10$ ps (Table 1). A dielectric structure with the dielectric thickness of 100 μm and a 5 mm half-gap would produce a longitudinal wake with a characteristic frequency of 100 GHz, or $\lambda/\sigma_z = 1$. Assuming a 30 cm length the wake

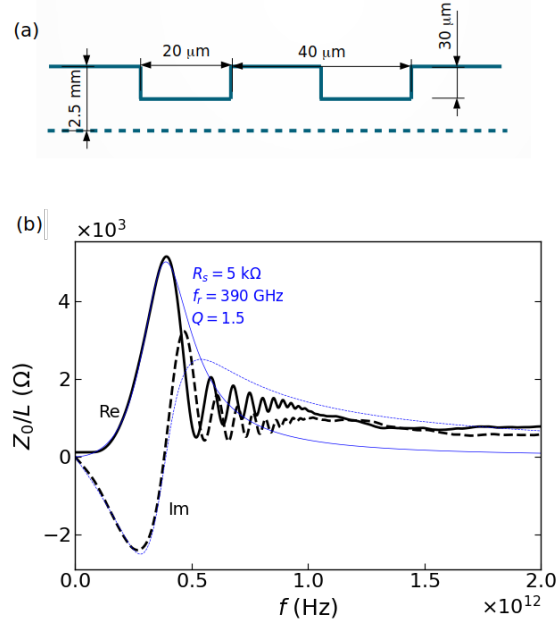


Figure 6. (a) the profile of the corrugated structure (not to scale). Dashed line shows the beam axis. (b) the longitudinal impedance per unit length. Blue lines represent a fit with a single-mode broadband resonator model.

Table 1. Key parameters used for the study with a 400 GHz corrugated and a 100 GHz dielectric structures

Structure	Corrugated	Dielectric
Ring circumference	110 m	110 m
Bunch energy	1.3 GeV	1.3 GeV
Bunch charge	300 – 700 pC	300 – 700 pC
Momentum compaction	5×10^{-4}	8×10^{-3}
Bunch length, rms	3 ps	10 ps
Synchrotron tune	0.0023	0.005
Structure length	30 cm	30 cm
Central frequency	390 GHz	100 GHz
Half-gap	2.5 mm	5 mm

strength is $W_0 = 4 \times 10^{14}$ V/pC, or $\kappa \approx 30$. We simulated numerically the process of slow adiabatic closure of the structure gap of 20 mm, where its wake is negligible, to 5 mm (Fig. 7a). As the gap is closed an initially Gaussian bunch transitions to a new equilibrium state with about 20% smaller rms bunch length (Fig. 7b). This greatly boosts the bunch's high frequency spectral components. Figure 7c shows a comparison of the initial and the final bunch power spectra: the components close to 100 GHz are enhanced by an order of magnitude.

It is convenient to characterize the temporal structure of the bunch in terms of the bunch form factor (BFF). The BFF is commonly used to characterize the performance of accelerator-based

radiation source [31]. In 1D it is computed as

$$\tilde{F}(\omega)^2 = \frac{1}{N^2} \left(\left| \sum_{i=0}^N \cos \frac{\omega z_i}{c} \right|^2 + \left| \sum_{i=0}^N \sin \frac{\omega z_i}{c} \right|^2 \right), \quad (4.2)$$

where z_i stand for individual positions of the macroparticles. The observed shortening of the bunch greatly increases the BFF at high frequencies. The boost is at least an order of magnitude at the frequencies above 40 GHz (Fig. 8).

A further decrease of the bunch length does not seem to be feasible as a larger wake strength leads to a longitudinal instability. This results in an increase of the bunch length, as seen, for example, by the drop of the BFF at high frequencies when increasing the bunch charge above 400 pC (Fig. 8).

Accessing even higher frequencies, on the order of 100 GHz, requires shorter bunches. Let us now consider the case of $\alpha = 5 \times 10^{-4}$, when the rms bunch length $\sigma_{z,0}/c = 3$ ps. A 30-cm-long corrugated structure can be installed in the same straight section. Considering the profile and impedance shown in Fig. 6 we obtain again a ratio $\lambda/\sigma_z \approx 1$. At the smallest gap of 5 mm the structure would generate a 5-10% increase of the peak current for the operational range of bunch charges between 400 and 700 pC (Fig. 9a). If the length of the structure can be increased or, alternatively, its gap reduced the amplification of the peak current can be even larger (seen in the plot as a hypothetical 2000 pC line). The bunch shortening, as expected, boosts the bunch form factor at higher frequencies, above 100 GHz (Fig. 9b).

In all the simulations for the combination of available aperture and structure length we stayed below the MWI threshold. On the other hand, our tracking studies with the single mode structure indicates a potential 30% increase of peak current before the impedance of the structure starts

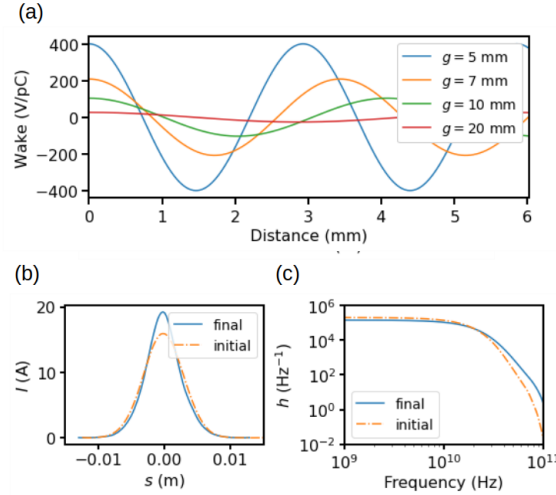


Figure 7. a – longitudinal wake potential created by a dielectric slab structure vs its half-opening g ; b – particle tracking shows how, as the gap of the structure is closed, the electron storage ring the bunches are compressed by 20%; c – power spectrum density; the spectral density at the structure’s eigenfrequency 100 GHz increases by an order of magnitude. Bunch charge $Q = 400$ pC.

triggering the MWI (Fig. 5). If the MWI can be avoided, for example, with the use of a longitudinal feedback or damping wigglers, the bunching could potentially be even greater.

In comparison, achieving a similar 20 – 30% increase in the peak current (shown in Fig. 5) by using a conventional rf-based approach would require increasing the voltage by 40 – 60%, as the bunch length scales as $\sigma_z \propto 1/\sqrt{V_{rf}}$. Alternatively, one can reduce the momentum compaction, α , of the lattice. On the other hand, this might compromise the beam stability as the thresholds of the microwave instability and the transverse mode coupling instability are proportional to α , while the rms bunch length – $\sigma_z \propto \sqrt{\alpha}$. Therefore, employing passive structures for bunching might be an appealing option.

4.4 PETRA IV ring example

As another practical example, let us consider a state-of-the art synchrotron light source PETRA IV that is currently being planned at DESY [32]. This 2304-m-long ring has a beam energy of 6 GeV and is capable of circulating trains of electron bunches with beam currents up to 200 mA. In the brightness operation mode the ring stores trains of 40-ps-long (rms) 1 nC bunches with a bunch spacing of 4 ns (Table 2). Thanks to its high energy physics heritage, the ring has four long and four short straight sections suitable for installation of additional components.

The equilibrium bunch length in the ring varies depending on the bunch intensity and the 3rd harmonic cavity voltage. The shortest bunch length that can be achieved in the ring without using its 3rd harmonics system is about 5 ps (1.5 mm) at low beam intensity [32].

For this example we considered a low intensity bunch of 400 pC and tracked it for 20000 turns (about 100 synchrotron periods), slowly increasing the wake strength. The wake was created by a hypothetical dielectric structure that could be installed in one of the ring’s unused undulated cells. The length of the structure was varied from 0 to 5 m (length of the standard undulator), while its half-gap was fixed at 5 mm. We note that a similar wake can also be produced with a corrugated structure (as shown in the previous section). As the wake strength increased (with the 3rd harmonic cavity turned off) the bunch length decreased until eventually the bunch became longitudinally unstable. The maximum bunch compression was achieved for the structure length of 2.25 m, corresponding to the wake strength $\kappa = 13.2$. The maximum bunch compression in this case amounted to a 10% increase in the peak current density, consistent with the prediction of the compression limit for $\lambda/\sigma_{z,0} = 1.2$ (Fig. 5). A higher compression can be achieved with a higher frequency structure, which would have to be longer, as discussed in section IV A.

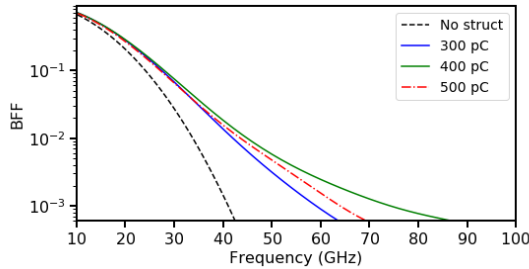


Figure 8. Bunch form factor can be increased at higher frequencies when using the corrugated structure. Different lines correspond to different bunch intensities.

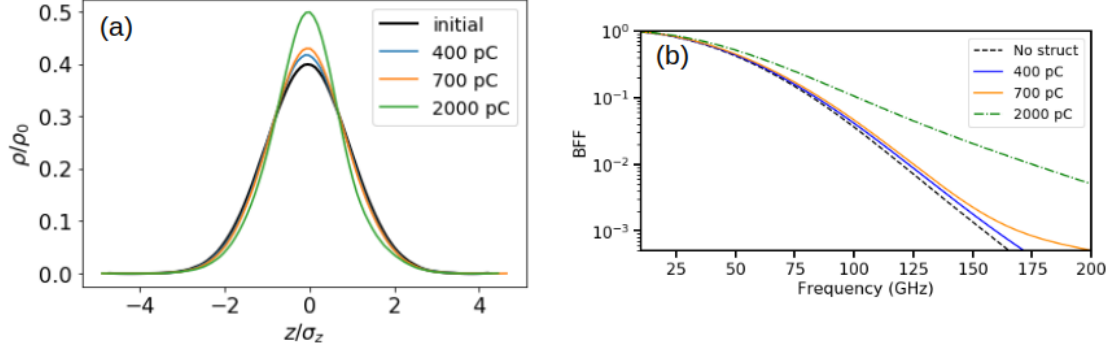


Figure 9. Bunch shortenings that can be obtained with a 30-cm-long 400 GHz corrugated structure in the KARA ring for different bunch charges (a) and the corresponding bunch form factors (b). The initial bunch length is assumed to be 0.9 mm, rms (shown as black lines).

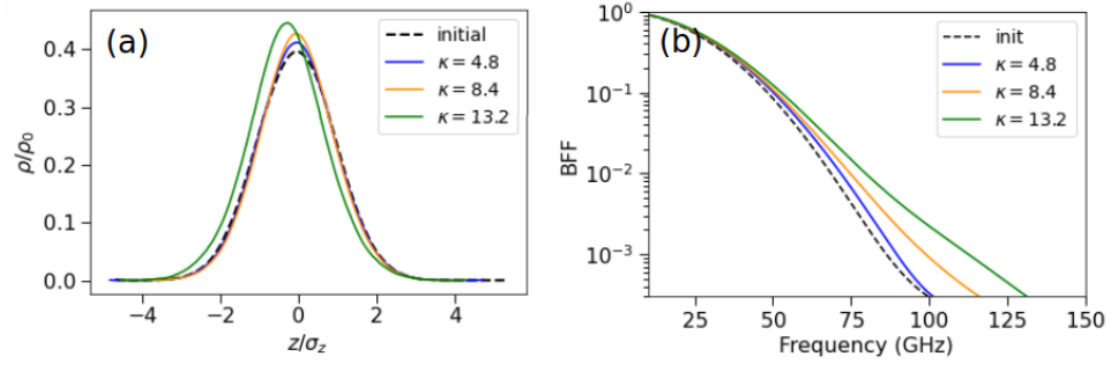


Figure 10. Bunch compression (a) and bunch form factor (b) for different wake strength in PETRA IV.

5 Radiation generation

After the bunch length has been reduced to increase the high-frequency spectral components the radiation at the desired frequency can be out-coupled using a separate, dedicated structure.

Table 2. PETRA IV parameters used for the study

Ring circumference	2304 m
Bunch energy	6.0 GeV
Bunch charge	400 pC
Momentum compaction	3.33×10^{-5}
Bunch length, rms	5 ps
Momentum spread, rms	9×10^{-4}
Synchrotron tune	0.005
Structure length	25 – 500 cm
Central frequency	160 GHz
Half-gap	5 mm

According to [14], the energy radiated at a given frequency E_{rad} is proportional to the BBF:

$$E_{rad} = N_b^2 e^2 \tilde{F}^2 L K_{||}, \quad (5.1)$$

where L stands for the structure length and $K_{||}$ is the loss factor, i.e. the total energy loss per meter of a charged particle travelling through the structure. Thus, an order of magnitude increase in \tilde{F}^2 results in a significant increase energy E_{rad} radiated at that frequency.

To illustrate the benefit of the proposed bunch compression scheme let us consider the hypothetical case depicted by green lines in Fig. (9): an initially 3 ps rms bunch is compressed until its peak current density increases by 20%. Let's assume now there is a second structure to out-couple the radiation at 100 GHz. Let it be a 10-cm-long dielectric structure similar to the one considered in section IV C. Initially, a part of the bunch loses the energy to the wakefield, while an almost equal part gains, making the total energy loss, and consequently the radiated power small (Fig. 11a). As the current profile changes under the action of the wakefield, its peak density aligns with the minimum of the wake potential and a larger fraction of the beam enters the region of negative wake potential, where particles lose energy (Fig. 11b) on each passage. This results in a four-fold increase of the beam energy being emitted in the 100 GHz structure: from 8×10^{-8} to 3×10^{-7} J per passage, or in terms of average radiation power, from 200 to 800 mW.

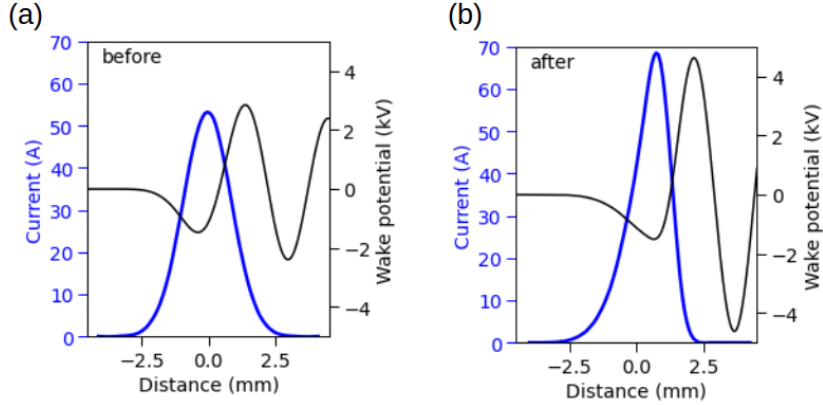


Figure 11. Wake potential of a hypothetical 100 GHz structure for the initial Gaussian bunch (a) and after compression (b) together with the corresponding current profiles. Before compression the energy loss per turn in the structure, defined as the product of the two curves, is negligible and increases dramatically as the bunch is compressed.

For the PETRA IV case described in section IV D the increase in the radiated power at 100 GHz would be four-fold: from 3×10^{-9} J to 2.3×10^{-8} J with the same 10-cm-long dielectric structure. The power radiated at 100 GHz could thus reach as much as 1.4 W with the full filling of 1920 bunches, circulating at 130 kHz, providing an effective repetition rate of 250 MHz. In comparison, a dedicated linac to produce THz, TELBE [33], delivers pulses of $\sim 1 \mu\text{J}$ at 50 kHz, or ~ 0.05 W.

6 Conclusion and Outlook

We have demonstrated that a dielectric or a corrugated structure can be used to compress the bunch length in a storage ring in a controllable way which is more efficient than conventional RF-based approaches. To do this one can use a structure with a characteristic wavelength $\lambda \sim \sigma$ that creates a wake potential that produces longitudinal focusing. Numerical simulations performed for the parameters of the KARA ring show that levels of 10-20% bunch shortening can be realistically achieved before encountering the microwave instability. Similar levels of additional bunch compression could be achieved in 4th generation light sources, operating at low momentum compaction factors, such as the planned PETRA IV. While the achievable shortening is moderate, this decrease of bunch length can boost the bunch form factor at the frequencies ~ 0.1 THz by up to an order of magnitude. This results in a significant increase of radiation power that can be extracted from the beam at those frequencies. Additional use of 3rd harmonic cavities at 1.5 GHz could be explored in the PETRA IV case to further reduce the bunch length in a similar fashion as the proposed CIRCE [5].

The outcoupling of microwave radiation can be done in a fashion similar to the MLS or UVSOR-II setups [34, 35], but utilizing the high total beam current of state-of-the-art light sources the average THz radiation power can be an order of magnitude larger: 800 mW for our PETRA IV case vs 60 mW at MLS. While the energy per pulse of ~ 10 μ J is smaller than ~ 1 mJ that can be achieved at an FEL [36, 37], in a storage ring one can obtain a high average power, high repetition rate, broadband source of THz-range radiation. This might be attractive for pump-probe spectroscopy experiments.

The required wakes can be realistically achieved with compact dielectric or corrugated structures. Slab structures particularly are attractive in this context because they can provide control over both the wake amplitude and, partially, the mode frequency. In addition, a more sophisticated corrugated waveguide with several rows of corrugation placed in parallel would provide a tunable frequency by exposing the beam to the different corrugated patterns. This could be appealing for generating short wavelength microwave radiation in synchrotron light sources. We also note that a reduction of bunch lengths can be contemplated for luminosity improvement of future and existing colliders.

Acknowledgments

We are grateful to the KARA team, in particular to Michael Nasse, Miriam Brosi, Markus Schwarz, for multiple discussions of ring parameters that were beneficial for producing realistic calculations of bunch shortening.

References

- [1] J.M. Byrd, W.P. Leemans, A. Loftsdottir, B. Marcelis, M.C. Martin, W.R. McKinney et al., *Observation of broadband self-amplified spontaneous coherent Terahertz synchrotron radiation in a storage ring*, *Phys. Rev. Lett.* **89** (2002) 224801.
- [2] M. Venturini and R. Warnock, *Bursts of coherent synchrotron radiation in electron storage rings : A Dynamical model*, *Phys. Rev. Lett.* **89** (2002) 224802.

- [3] E. Roussel et al., *Microbunching Instability in Relativistic Electron Bunches: Direct Observations of the Microstructures Using Ultrafast YBCO Detectors*, *Phys. Rev. Lett.* **113** (2014) 094801.
- [4] M. Abo-Bakr, J. Feikes, K. Holldack, P. Kuske, W.B. Peatman, U. Schade et al., *Brilliant, Coherent Far-Infrared (THz) Synchrotron Radiation*, *Phys. Rev. Lett.* **90** (2003) 094801.
- [5] J. Byrd, M.C. Martin, W. McKinney, D. Munson, H. Nishimura, D. Robin et al., *Circe: a dedicated storage ring for coherent thz synchrotron radiation*, *Infrared Physics & Technology* **45** (2004) 325.
- [6] C. Evain et al., *Coherent Terahertz synchrotron radiation mastered by controlling the irregular dynamics of relativistic electron bunches*, *Nature Phys.* **15** (2019) 635 [[1810.11805](#)].
- [7] G.L. Carr, M.C. Martin, W.R. McKinney, K. Jorda, G.R. Neil and G.P. Williams, *High power terahertz radiation from relativistic electrons*, *Nature* **420** (2002) 153.
- [8] S. Antipov, M. Babzien, C. Jing, M. Fedurin, W. Gai, A. Kanareykin et al., *Subpicosecond Bunch Train Production for a Tunable mJ Level THz Source*, *Phys. Rev. Lett.* **111** (2013) 134802.
- [9] F. Lemery and P. Piot, *Ballistic Bunching of Photoinjected Electron Bunches with Dielectric-Lined Waveguides*, *Phys. Rev. ST Accel. Beams* **17** (2014) 112804 [[1407.1005](#)].
- [10] G. Andonian, S. Barber, F.H. O'Shea, M. Fedurin, K. Kusche, C. Swinson et al., *Generation of Ramped Current Profiles in Relativistic Electron Beams Using Wakefields in Dielectric Structures*, *Phys. Rev. Lett.* **118** (2017) 054802.
- [11] F. Lemery et al., *Passive Ballistic Microbunching of Nonultrarelativistic Electron Bunches Using Electromagnetic Wakefields in Dielectric-Lined Waveguides*, *Phys. Rev. Lett.* **122** (2019) 044801 [[1806.09513](#)].
- [12] F. Mayet, R. Assmann and F. Lemery, *Longitudinal phase space synthesis with tailored 3D-printable dielectric-lined waveguides*, *Phys. Rev. Accel. Beams* **23** (2020) 121302 [[2009.12123](#)].
- [13] B.D. O'Shea et al., *Observation of acceleration and deceleration in gigaelectron-volt-per-metre gradient dielectric wakefield accelerators*, *Nature Commun.* **7** (2016) 12763.
- [14] K. Floetmann, F. Lemery, M. Dohlus, M. Marx, M. Ivanyan and V. Tsakanov, *Superradiant Cherenkov-Wakefield radiation as THz source for FEL facilities*, [2005.05640](#).
- [15] M. Kellermeier, F. Lemery, K. Floetmann, W. Hillert and R. Assmann, *Self-calibration technique for characterization of integrated THz waveguides*, *Phys. Rev. Accel. Beams* **24** (2021) 122001 [[2104.01401](#)].
- [16] J. Haissinski, *Exact longitudinal equilibrium distribution of stored electrons in the presence of self-fields*, *Nuovo Cim. B* **18** (1973) 72.
- [17] Y. Shobuda and K. Hirata, *The Existence of a static solution for the Haissinski equation with purely inductive wake force*, *Part. Accel.* **62** (1999) 165.
- [18] C. Thomas, R. Bartolini, J.I.M. Botman, G. Dattoli, L. Mezi and M. Migliorati, *An analytical solution for the haissinski equation with purely inductive wake fields*, *Europhysics Letters* **60** (2002) 66.
- [19] A.V. Burov, *BUNCH LENGTHENING: IS IT INEVITABLE?*, *Part. Accel.* **28** (1990) 47.
- [20] A.V. Burov and A.V. Novokhatsky, *The Device for bunch selffocusing*, in *4th Advanced ICFA Beam Dynamics Workshop: Collective Effects in Short Bunches*, 2, 1990.
- [21] K.L. Bane, M.H.R. Donald, A. Hofmann, J.M. Jowett, W.S. Lockman, P.L. Morton et al., *BUNCH LENGTH AND IMPEDANCE MEASUREMENTS IN SPEAR*, *Conf. Proc. C* **880607** (1988) 878.

- [22] K.L. Bane, *Bunch lengthening in the SLC damping rings*, Tech. Rep. [SLAC-PUB-5177](#), SLAC, Stanford, CA (1990).
- [23] A. Gerasimov, *Longitudinal Wakefield Focusing: An Unconventional Approach to Reduce the Bunch Length in Tevatron*, Tech. Rep. FERMILAB-FN-62XX, Fermilab, Batavia, Illinois (1994).
- [24] E. Metral, *Longitudinal microwave instability in lepton bunches*, *Conf. Proc. C* **030512** (2003) 3047.
- [25] A. Hofmann, *Single Beam Collective Phenomena: Longitudinal*, .
- [26] M. Rosing and W. Gai, *Longitudinal and Transverse Wake Field Effects in Dielectric Structures*, *Phys. Rev. D* **42** (1990) 1829.
- [27] K.-Y. Ng, *Wake Fields in a Dielectric Lined Waveguide*, *Phys. Rev. D* **42** (1990) 1819.
- [28] P. Piot, J. Wang and F. Lemery, “Diwakecyl.” <https://github.com/NIUaard/DiWakeCyl>.
- [29] A. Tremaine, J. Rosenzweig and P. Schoessow, *Electromagnetic wake fields and beam stability in slab-symmetric dielectric structures*, *Phys. Rev. E* **56** (1997) 7204.
- [30] I. Zagorodnov, *Computation of Electromagnetic Fields Generated by Relativistic Beams in Complicated Structures*, in *2nd North American Particle Accelerator Conference*, p. WEA1IO02, 2017, [DOI](#).
- [31] J.S. Nodvick and D.S. Saxon, *Suppression of Coherent Radiation by Electrons in a Synchrotron*, *Phys. Rev.* **96** (1954) 180.
- [32] K. Wittenburg, *PETRA IV: Upgrade of PETRA III to the Ultimate 3D X-ray Microscope* (10, 2019), [10.3204/PUBDB-2019-03613](#).
- [33] B. Green, S. Kovalev, V. Asgekar, G. Geloni, U. Lehnert, T. Golz et al., *High-field high-repetition-rate sources for the coherent thz control of matter*, *Scientific Reports* **6** (2016) 22256.
- [34] A. Pohl, A. Hoehl, R. Müller, G. Ulm, M. Ries, G. Wüstefeld et al., *Terahertz pump-probe experiment at the synchrotron light source mls*, in *2013 38th International Conference on Infrared, Millimeter, and Terahertz Waves (IRMMW-THz)*, pp. 1–2, 2013, [DOI](#).
- [35] S. Kimura, E. Nakamura, M. Hosaka, T. Takahashi and M. Katoh, *Design of Terahertz Pump—Photoemission Probe Spectroscopy Beamline at UVSOR-II*, *AIP Conference Proceedings* **1234** (2010) 63
[https://pubs.aip.org/aip/acp/article-pdf/1234/1/63/11959734/63_1_online.pdf].
- [36] Y. Choporova, V. Gerasimov, B. Knyazev, S. Sergeev, O. Shevchenko, R. Zhukavin et al., *First terahertz-range experiments on pump – probe setup at novosibirsk free electron laser*, *Physics Procedia* **84** (2016) 152.
- [37] Z. Zhang, A.S. Fisher, M.C. Hoffmann, B. Jacobson, P.S. Kirchmann, W.-S. Lee et al., *A high-power, high-repetition-rate THz source for pump–probe experiments at Linac Coherent Light Source II*, *Journal of Synchrotron Radiation* **27** (2020) 890.